The Physics of Chromospheric Plasmas
ASP Conference Series, Vol. 368, 2007
Petr Heinzel, Ivan Dorotovič and Robert J. Rutten, eds.

Full-Stokes Observations and Analysis of He I 10830 Å in a Flaring Region

Clementina Sasso[1], Andreas Lagg[1], Sami K. Solanki[1],
Regina Aznar Cuadrado[1] and Manuel Collados[2]

[1] *MPI für Sonnensystemforschung, Katlenburg-Lindau, Germany*
[2] *Instituto de Astrofísica de Canarias, La Laguna, Spain*

Abstract. We present observations of the full Stokes vector in a flaring region, taken in the chromospheric He I 10830 Å multiplet. The data were recorded with the new Tenerife Infrared Polarimeter (TIP 2) at the German Vacuum Tower Telescope (VTT) during May 2005. The He profiles during the flare are extraordinary, showing extremely broad Stokes I absorption and very complex and spatially variable Stokes V signatures. We give first results on the line-of-sight velocities and the magnetic field vector values in the chromosphere for one observed Stokes profile by applying an inversion code to the He I lines.

1. Introduction

The He I 10830 Å multiplet is a powerful diagnostic of the solar chromospheric magnetic and velocity field. The components of the He I multiplet are sensitive to the Zeeman effect and therefore these lines are suitable for spectropolarimetric measurements of the magnetic field vector in the upper chromosphere, where they are formed (Trujillo Bueno et al. 2002; Solanki et al. 2003).

The He I 10830 Å multiplet originates between the atomic levels 2^3S_1 and $2^3P_{2,1,0}$. It comprises a "blue" component at 10829.09 Å with $J_u = 0$ (Tr1), and two "red" components at 10830.25 Å with $J_u = 1$ (Tr2) and at 10830.34 Å with $J_u = 2$ (Tr3), which are blended at solar chromospheric temperatures.

2. Observations

The data we present here were recorded with the German Vacuum Tower Telescope (VTT) with the new Tenerife Infrared Polarimeter (TIP 2; Collados et al. 2007) at the Teide Observatory in Tenerife. During observations on 2005 May 18, a flare of GOES class C2.0 erupted in the west part of the active region NOAA 10763, located at 24° W, 14° S on the solar disc. The active region was covered by scanning in steps of 0.35″ perpendicular to the slit orientation from 14:38:29 to 15:02:26 UT. In the scanned region a filament and the flare ribbons were visible in the Hα slit jaw camera images. The spectral dispersion of the instrument is 15 mÅ per pixel. The spectral window (10825 – 10836 Å) contains four photospheric lines of Si I at 10827.1 Å, Ca I at 10829.3 and 10833.3 Å and Na I at 10834.8 Å, the chromospheric He I multiplet and two telluric blends at

10832.1 Å and 10833.9 Å. Figure 1 displays Stokes I maps for the observed region in the continuum and in the core of the "red" components of the He I lines.

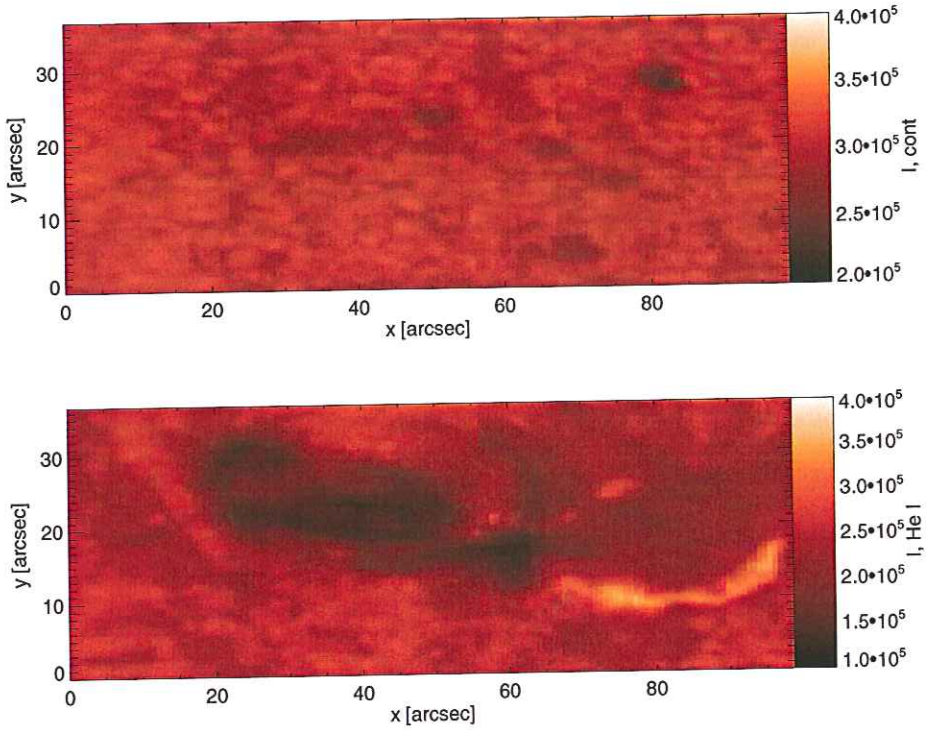

Figure 1. Intensity maps of the active region NOAA 10763 (24° W, 14° S) obtained at different wavelength regions. *Top*: Continuum. *Bottom*: He I line core of the "red" component.

From the lower map of Fig. 1 the presence of a strong absorption in the He lines is clearly visible during the central part of the scan. At the end of the scan, the lines show a completely different behaviour and show less absorption then in the quiet sun, at $y \approx 8'' - 15''$ ($65'' < x < 98''$). The analysis of the He Stokes profiles observed during the scan reveals huge differences in the profile shape. In Fig.2 we present some examples of observed Stokes I profiles at different pixel positions. In all the profiles we can notice the presence of different atmospheric components for the He lines (see Sect. 3) which are blue- or redshifted, implying upflows or downflows. In some profiles of Fig. 2, e.g., (b) and (c), blueshifted and redshifted components of the He multiplet coexist. Another example is shown in Fig. 3 (black lines) the Stokes vector at pixel position $x = 64''$, $y = 15''$ of Fig. 1. The spectra are binned over four spectral pixels and eight spatial pixels in order to increase the signal-to-noise level. The I profile shows a very broad absorption affecting the wavelength range 10829 Å to 10835 Å and in the Stokes V profile we see the signature of several magnetic components within this range. We observe an unusually wide range of Stokes profiles at several locations of the scan.

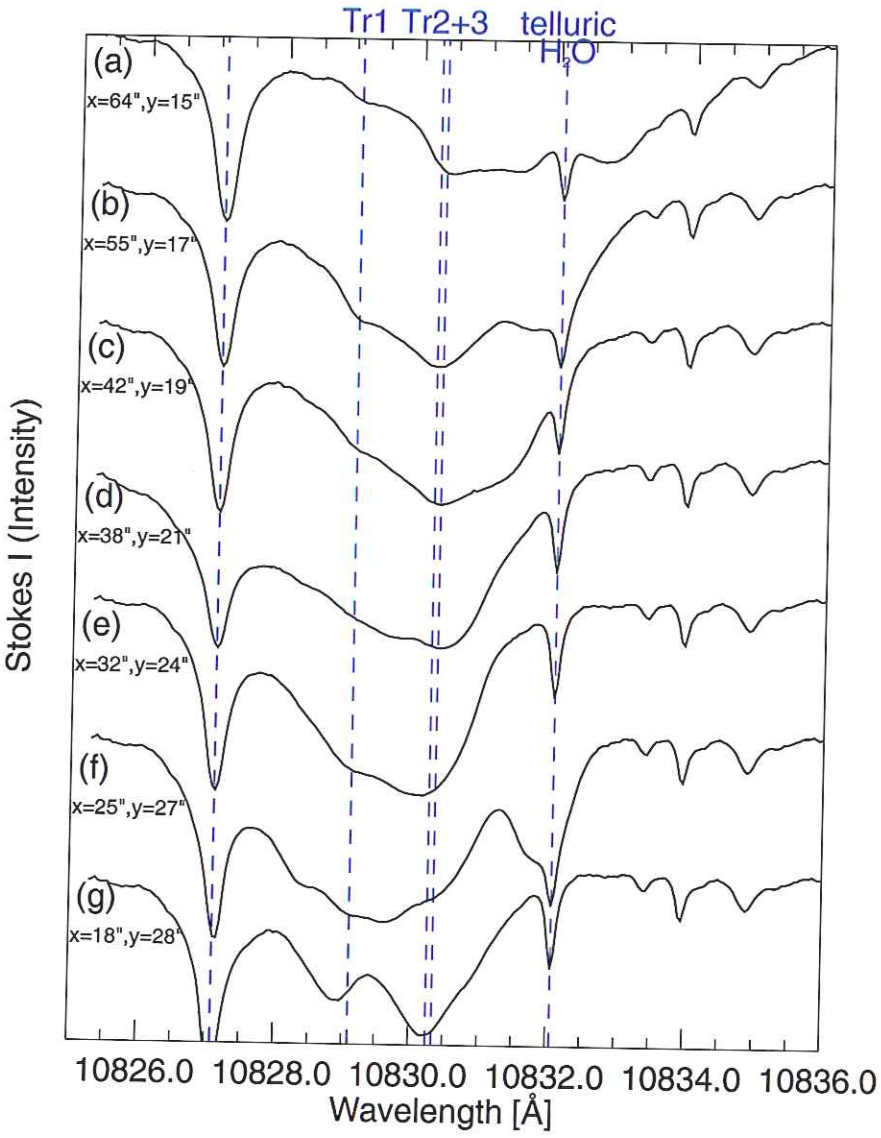

Figure 2. Examples of the observed Stokes I profiles, with their pixel positions marked on their left side.

3. Inversions of the Stokes Vector

In order to retrieve the full magnetic field vector and the velocity along the line-of-sight, we analyze the chromospheric He I lines with an inversion involving the forward calculations of the four Stokes profiles. The He I lines show a complex non-LTE formation but due to their optical thinness, their narrowness and the absence of any significant photospheric contributions, these lines can be used to deduce the magnetic field vector and the line-of-sight velocity at the height of

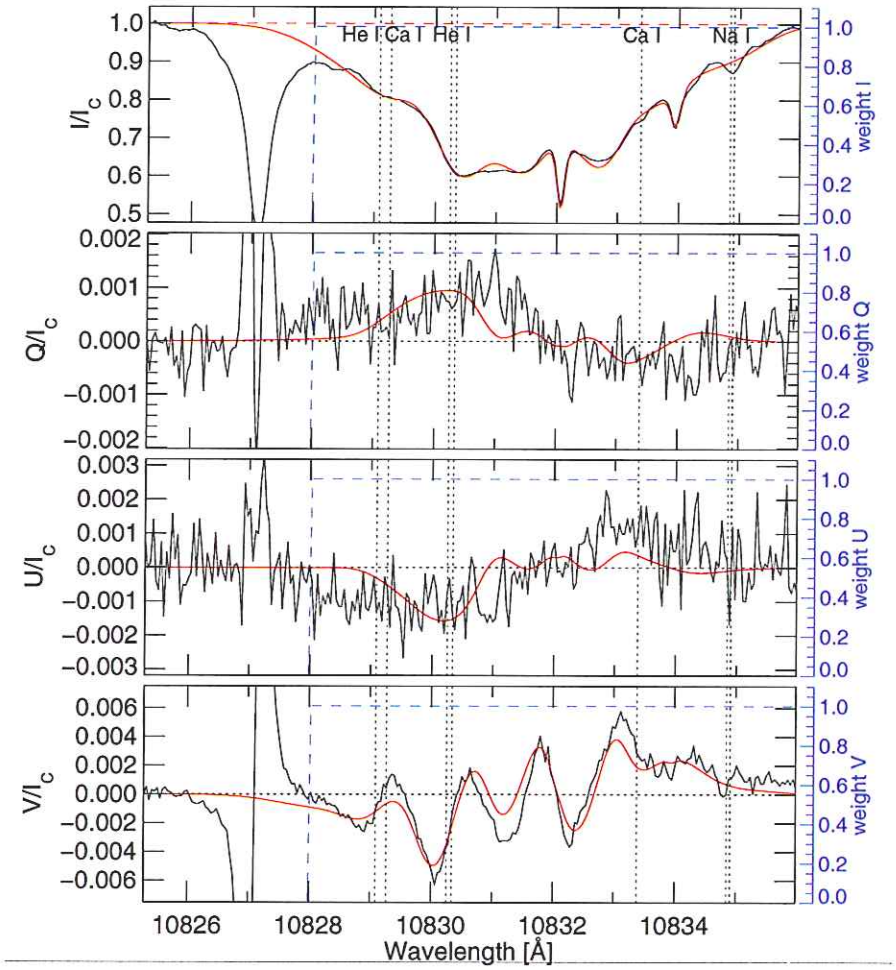

Figure 3. Inversions of the Stokes I, Q, U and V at position $x = 64''$, $y = 15''$ of Fig. 1. The black thick lines are the observed profiles while the thin (red in the electronic version) lines are the fits obtained considering, as input to the inversion code, three coupled magnetic components of the He I lines.

formation without the need to understand the details of their formation (Rüedi et al. 1995).

We apply to the spectropolarimetric data the numerical code for the synthesis and inversion of Stokes profiles in a Milne-Eddington atmosphere described by Lagg et al. (2004). This inversion method was extended to take into account the effect of incomplete Paschen-Back splitting following Socas-Navarro et al. (2005) and Sasso et al. (2006). Here we present, in particular, the inversion of the full Stokes vector in the He I 10830 Å multiplet, at pixel position $x = 64''$, $y = 15''$ of the maps in Fig. 1. In order to obtain a good fit to the observations, we had to consider 3 different atmospheric components for the He I lines. The

components have the same magnetic field vector, but different velocities along the line-of-sight. The best fit shown in Fig. 3 reproduces the observed Stokes vector reasonably well. A sufficient good 3-component fit of these profiles is obtained for a single magnetic component with a $\approx$ 380 G, an inclination to the vertical of 116° and an azimuth of 60°. The different components do show strongly different line shifts, however. The fit identifies a component almost at rest and two fast components with supersonic velocities of 36 and 64 km/s. Such profiles displaying 3 atmospheric components are reasonably common and we have even found cases which require 4 atmospheric components to be reproduced.

4. Discussion

From the analysis of the observed profile discussed in Sect. 3, and of other profiles not presented in this paper, we have evidence for the presence of different unresolved atmospheric components for the He lines, coexisting in the same resolution element. Multiple unresolved atmospheric components are also found in non-flaring regions (Lagg et al. 2006), but they are more common and in particular three or more components are often needed. Some times supersonic upflows and downflows of the He I lines appear in the same pixel. We have also evidence of different He components showing emission and absorption within the same profile. The shifts for most of the profiles are associated with supersonic velocities. In particular, we measure upflows with velocities up to 40 km/s and downflows with velocities up to 64 km/s.

In addition to completing the inversion of the whole map we plan to investigate the connection between the flare, happening at coronal heights, and what we observe at chromospheric levels.

References

Collados M., Lagg A., Díaz García J. J, Hernández Suárez E., López López R., Páez Mañá E., Solanki S. K., 2007, in P. Heinzel, I. Dorotovic, R. J. Rutten (eds.) The Physics of Chromospheric Plasmas, ASP Conf. Series, these proceedings

Lagg A., Woch J., Krupp N., Solanki S. K., 2004, A&A 414, 1109

Lagg A., Woch J., Solanki S. K., Krupp N., 2006, A&A, in press

Rüedi I., Solanki S. K., Livingston W. C., 1995, A&A 293, 252

Sasso C., Lagg A., Solanki, S. K., 2006, A&A 456, 367

Socas-Navarro H., Trujillo Bueno J., Landi Degl'Innocenti E., 2005, ApJS 160, 312

Solanki S. K., Lagg A., Woch J., Krupp N., Collados M., 2003, Nat 425

Trujillo Bueno J., Landi Degl'Innocenti E., Collados M., Merenda L., Manso Sainz R., 2002, Nat 415, 403